Mobility of Free Ends and Junction Points in a Lamellar Block Copolymer

Türkan Haliloğlu, R. Balaji, and Wayne L. Mattice*

Institute of Polymer Science, The University of Akron, Akron, Ohio 44325-3909

*Received September 17, 1993; Revised Manuscript Received December 3, 1993**

ABSTRACT: The dynamics of diblock copolymers organized into a lamellar microstructure has been simulated on a cubic lattice. The chains of $A_{10}B_{10}$ are present at a volume fraction of 0.847 and the reduced pairwise interaction energy between A and B is 0.5, which places the system near the microphase separation transition. Parallel simulations were performed in which the voids participated in no interactions with either block and in which they behaved as monomeric species of B. The motion is monitored for the beads at the free ends of both blocks and for the beads at the junction between the blocks. At short times, the beads at the free ends experience greater motion than the beads at the junction points. The trajectory was long enough to estimate the self-diffusion coefficient for the chains in the system where the voids do not participate in interactions with either block. This self-diffusion coefficient could be decomposed into components in the plane of the lamellae and normal to the interface. These components differ by an order of magnitude, with the slower diffusion being in the direction normal to the plane of the interface. The bond autocorrelation function decays quickly to zero for the bonds at the free ends, but it does not decay to zero on the time scale of the simulations for the bond at the junction between the two blocks.

Introduction

One of the interesting properties of diblock copolymers is their ability under the right conditions to spontaneously self-assemble into structures with various morphologies.[1] The dynamics of individual chains within these microstructures, after they have equilibrated, is attracting interest from theorists and experimentalists.[2-5] The nonuniformity of the local composition is expected to have a profound influence on the self-diffusion coefficient of the chains. A further complication occurs when the variations in the local composition are anisotropic, as in a lamellar structure. The mobility of a segment may depend on its location within the diblock copolymer, particularly under conditions of strong segregation. Then the ends of the chains may sample the entire structure, while the junctions between the blocks are strongly confined to the interfacial region.[6,7] The mobility of the free ends is controlled by entropic considerations, but the junctions between the blocks are controlled by stronger energetic restrictions which favor their confinement to the interfacial region.

Simulations of systems of diblock copolymers at high density (volume fraction of copolymer in the vicinity of 0.8) at or near the microphase separation transition have been developed recently.[8,9] Here we report the dynamics of the chains in a lamellar system, after the system has equilibrated. The data permit an estimate of the ratio of the self-diffusion coefficients parallel and perpendicular to the surface. They also reveal differences in the mobilities of the segments at the free ends and at the junction points.

Method

The simulation is based on the one described recently, where the focus was on the static properties (structure factor, mean-square dimensions, bond orientation autocorrelation functions) for systems above and slightly below the microphase separation transition temperature.[9]

The present simulations employ a cubic lattice, of size 22^3, with periodic boundary conditions in all directions. The diblock copolymer, $A_{10}B_{10}$, contains 10 beads of A and 10 beads of B. It is present at a volume fraction of 0.847. Reptation[10] and kink–jump bond motions[11] are used alternately to generate new structures, which are accepted according to the Metropolis rule.[12]

All simulations employ self-avoiding chains and a reduced pairwise interaction energy, ϵ_{AB}, that is applied whenever nonbonded segments of A and B are nearest neighbors. In every simulation, $\epsilon_{AB} > 0$. Another reduced pairwise interaction energy, denoted by ϵ_{AS}, is applied whenever a segment of A has a void as a nearest neighbor. All other pairwise interactions are always assigned as zero. Two numerical assignments were used for ϵ_{AS}. Those simulations that employ $\epsilon_{AS} = 0$ will be referred to as "dry", and those that employ $\epsilon_{AS} = \epsilon_{AB} > 0$ will be referred to as "wet". In the wet simulations, the voids behave as a low molecular weight solvent with the same energetics as a segment of B, but in the dry simulations, the voids have the energetics of a vacuum. After equilibration of the lamellar structures, the simulation was continued for computation of the trajectories that are the subject of the present work.

Mean-Square Displacements of Free Ends and Junction Points

A snapshot of the equilibrated wet system when $\epsilon_{AB} = 0.5$ is depicted in Figure 1. It depicts an example of the lamellae that form spontaneously in these simulations, when ϵ_{AB} is of an appropriate size. The transition from the disordered state to the lamellar structures occurs at ϵ_{AB} near 0.5.

The mean-square displacements of the beads that are located at the free ends and at the junctions of the two blocks have been calculated from the trajectories for the wet and dry systems using the following expressions:

$$r_a^2(\tau) = \frac{1}{N_c t_{run}} \sum_{i=1}^{N_c} \sum_{t=1}^{t_{run}} [r_{a,i}(\tau + t) - r_{a,i}(t)]^2 \qquad (1)$$

$$r^2(\tau) = \sum_a r_a^2(\tau) \qquad (2)$$

where $a = x, y$, and z for displacements along the x, y, and z axes, respectively. The z axis is normal to the interface of the lamellae. The number of chains is denoted by N_c,

* Abstract published in *Advance ACS Abstracts*, February 1, 1994.

0024-9297/94/2227-1473$04.50/0

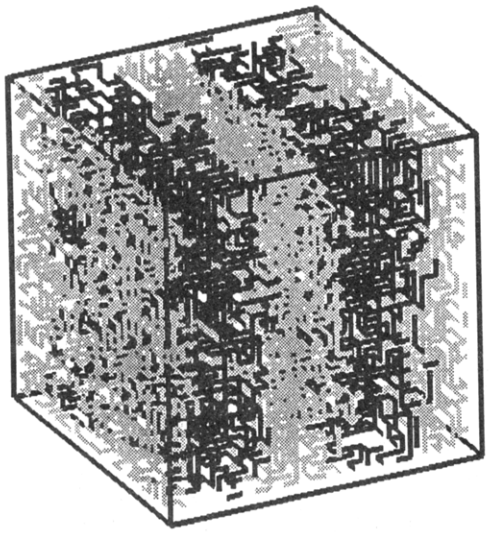

Figure 1. Snapshot of the periodic box for the equilibrated wet system with $\epsilon_{AB} = \epsilon_{AS} = 0.5$. The gray regions are domains of the insoluble blocks (A) and the black regions are domains of the soluble blocks (B). The voids are not shown.

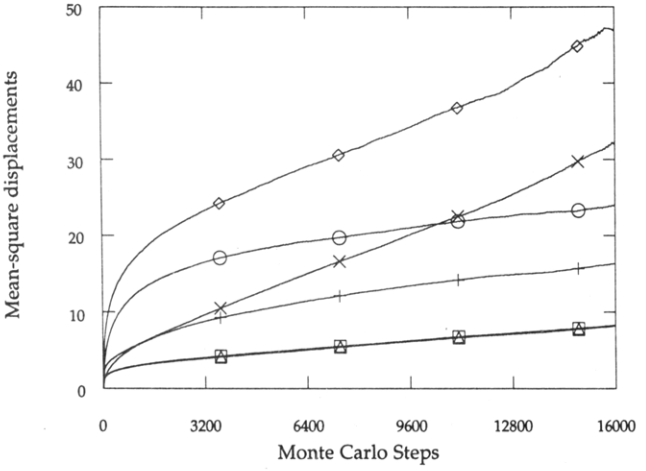

Figure 2. $r^2(\tau)$, in squared lattice units, as a function of Monte Carlo time steps for the beads at the free ends and at the junctions between the blocks in the wet and dry systems. Dry system: (◇) free ends of either block; (×) beads at the junction of the two blocks. Wet system: (+) free ends of the insoluble block (A block); (△) A beads at the junctions with the B block; (□) B beads at the junctions with the A block; (○) free ends of the soluble block (B block). In this figure and in the remaining figures, the symbols serve only to identify the curves. They do not represent the complete set of data used for generation of the curves.

τ is the time interval between observations, expressed in Monte Carlo time steps, and t_{run} is the number of observations.

Figure 2 depicts $r^2(\tau)$ for the beads at the free ends and the beads at the junction between the blocks in the wet and dry systems when $\epsilon_{AB} = 0.5$. In this figure, and in the remaining figures, the symbols serve only to identify the curves. They do not represent the complete set of data used for the plotting of the curves. The two blocks must exhibit the same properties in the dry system, and for that reason only two curves are plotted for that system. However, in the wet system the A block may have different properties from the B block, and for that reason data for four beads in the wet system are plotted. Results show that the A and B beads at the junctions have the same $r^2(\tau)$, but the A and B beads at the free ends have readily distinguishable $r^2(\tau)$ in the wet system.

All six curves show a rapid rise at short times. This rise is larger for the beads at the free ends than for the beads at the junctions between the blocks (for a specified type of system) and larger for the dry system than for the wet system (for a specified type of bead). In the wet system, the beads at the ends of the soluble blocks experience a faster initial rise in $r^2(\tau)$ than do the beads at the ends of the insoluble blocks.

Table 1. Limiting Values of the Slope of Mean-Square Displacement vs Monte Carlo Time Step

system	bead	$\lim_{\tau\to\infty} dr^2(\tau)/d\tau^a$
dry	free end	2.1×10^{-3}
dry	junction	1.9×10^{-3}
wet	free end of A	0.41×10^{-3}
wet	junction	0.30×10^{-3}
wet	free end of B	0.41×10^{-3}

[a] In squared lattice units (Monte Carlo time step)$^{-1}$, using data from 10 000 to 16 000 Monte Carlo time steps. Uncertainties are about 0.1×10^{-3} for the dry system ($\epsilon_{AB} = 0.5$) and 0.05×10^{-3} for the wet system ($\epsilon_{AB} = \epsilon_{AS} = 0.5$).

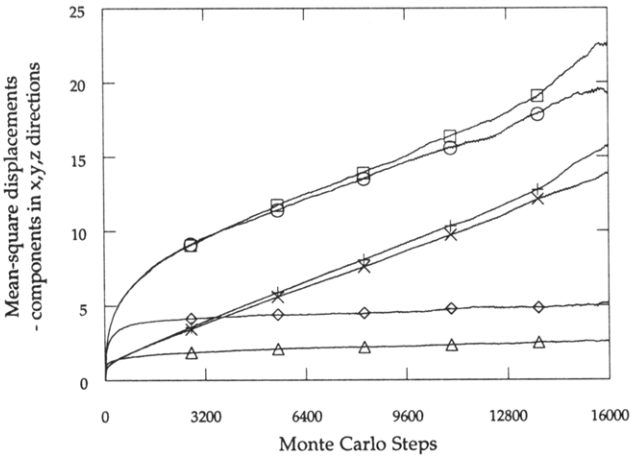

Figure 3. Decomposition of $r^2(\tau)$ from Figure 2 into $r_a^2(\tau)$ in the dry system. Beads at the free ends: (○) x component; (□) y component; (◇) z component. Beads at the junctions between the blocks: (×) x component; (+) y component; (△) z component.

At longer times, $r^2(\tau)$ approaches a behavior that is nearly linear in the number of Monte Carlo time steps. The six curves give an indication of separation into two groups, according to whether they belong to the wet or dry system, insofar as their limiting slopes are concerned. Table 1 presents the limiting slopes obtained from the data in the range of 10 000 to 16 000 Monte Carlo time steps. The diffusion coefficient is $^1/_6$ of these limiting slopes.

The limiting slopes are indistinguishable for the two types of beads in the dry system. This result, plus the good approximation to linear behavior at times longer than ~5000 Monte Carlo time steps, suggests that the limiting slopes can properly be identified with the self-diffusion coefficient of the chains. This interpretation is reinforced by the sizes of $r^2(\tau)$ at times longer than 10 000 Monte Carlo time steps. They are several multiples of the mean-square radius of gyration of the individual chains, which is 6–7 squared lattice units in these systems.[9]

The slower motion in the wet system probably arises because a positive ϵ_{AS} inhibits the motion of the A block, as compared to the case where $\epsilon_{AS} = 0$. In the wet system, the limiting values of the slopes from Figure 2 are a third again as large for the beads at the free ends as for the beads at the junctions between the blocks. Furthermore, the mean-square displacement of the beads at the junctions between the blocks does not become comparable in size to the mean-square radius of gyration (6–7) until ~10 000 Monte Carlo time steps. Results show that the self-diffusion coefficient of the chains is smaller in the wet

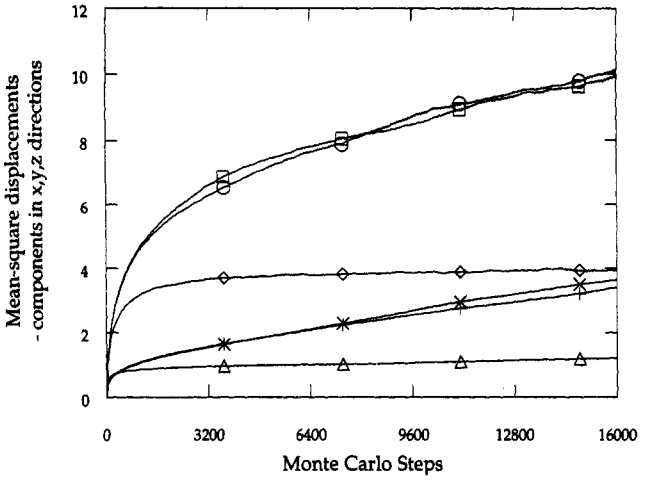

Figure 4. Decomposition of $r^2(\tau)$ from Figure 2 into $r_\alpha^2(\tau)$ for the soluble block in the wet system. Beads at the free ends: (○) x component; (□) y component; (◇) z component. Beads at the junctions between the blocks: (×) x component; (+) y component; (△) z component.

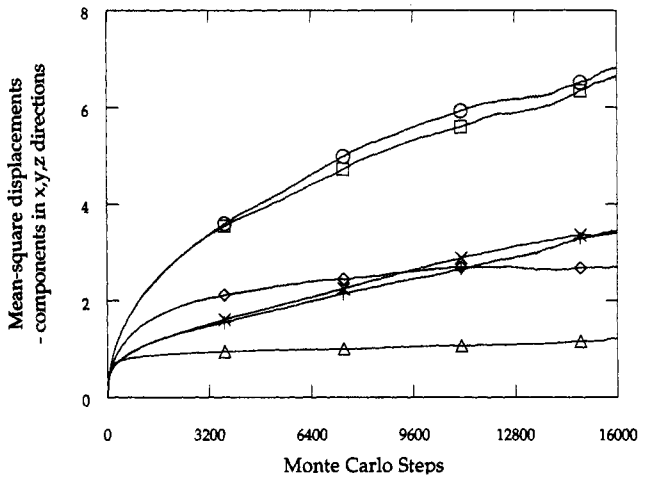

Figure 5. Decomposition of $r^2(\tau)$ from Figure 2 into $r_\alpha^2(\tau)$ for the insoluble block in the wet system. Beads at the free ends: (○) x component; (□) y component; (△) z component. Beads at the junctions between the blocks: (×) x component; (+) y component; (△) z component.

system than in the dry system, but exactly how much smaller is uncertain, because the diffusion coefficient in the wet system cannot be assigned unequivocally from the simulations. Probably the ratio of the self-diffusion coefficients in the dry and wet systems is in the range of 4–7, based on the ratios of comparable limiting slopes in Table 1.

The mean-square displacements are decomposed into their components along the three axes in Figures 3–5. For a given system and bead, $r_x^2(\tau)$ and $r_y^2(\tau)$ exhibit similar behavior throughout the trajectory, as expected. With the exception of the first few hundred Monte Carlo time steps, they are much larger than $r_z^2(\tau)$ for the same bead. Even after 16 000 Monte Carlo time steps, $r_z^2(\tau)$ has not reached the size of the mean-square radius of gyration (6–7). The sharpness of the interface between the domains and the average width of the domains themselves[9] justify this result.

The x, y, and z components of the limiting slopes, evaluated from the data in the range of 10 000–16 000 Monte Carlo time steps, are collected in Table 2. These limiting slopes suggest that the self-diffusion coefficient in the plane of the lamellae is an order of magnitude larger than the self-diffusion coefficient normal to that plane in the dry system, and the ratio might be of comparable size

Table 2. Decomposition of the Slope of the Mean-Square Displacements[a] vs Monte Carlo Time Steps

system	bead	$\lim_{\tau\to\infty} \frac{dr^2(\tau)}{d\tau}$	$\lim_{\tau\to\infty} \frac{dr_y^2(\tau)}{d\tau}$	$\lim_{\tau\to\infty} \frac{dr_z^2(\tau)}{d\tau}$
dry	free end	0.85×10^{-3}	1.21×10^{-3}	0.07×10^{-3}
dry	junction	0.83×10^{-3}	1.04×10^{-3}	0.05×10^{-3}
wet	free end of A	0.17×10^{-3}	0.20×10^{-3}	0.03×10^{-3}
wet	A at junction	0.12×10^{-3}	0.16×10^{-3}	0.02×10^{-3}
wet	B at junction	0.15×10^{-3}	0.13×10^{-3}	0.02×10^{-3}
wet	free end of B	0.20×10^{-3}	0.20×10^{-3}	0.02×10^{-3}

[a] In squared lattice units (Monte Carlo time step)$^{-1}$, using data from 10 000 to 16 000 Monte Carlo time steps. Uncertainties in the dry system ($\epsilon_{AB} = 0.5$) are about 0.2×10^{-3} for x and y and 0.02×10^{-3} for z. Uncertainties in the wet system ($\epsilon_{AB} = \epsilon_{AS} = 0.5$) are about 0.04×10^{-3} for x and y and 0.01×10^{-3} for z.

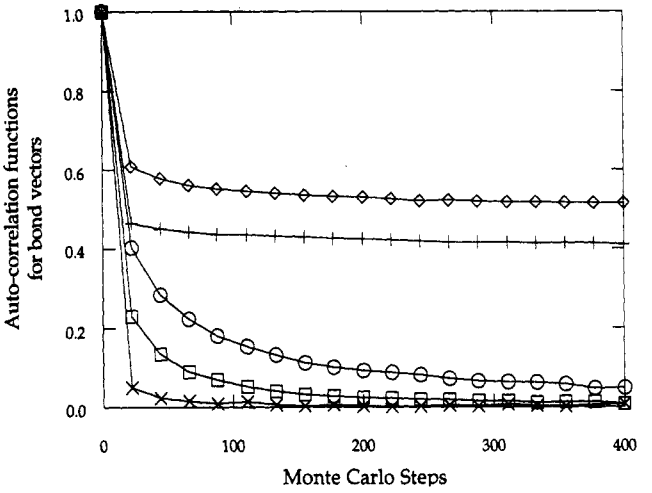

Figure 6. Decay of $M(\tau)$ at short times for the selected bonds when $\epsilon_{AB} = 0.5$ or $\epsilon_{AB} = \epsilon_{AS} = 0.5$. Dry system: (×) bond at the free end of one of the blocks; (+) bond at the junction between the blocks. Wet system: (○) bond at the free end of the insoluble blocks (A blocks); (□) bond at the free end of the soluble blocks (B blocks); (◇) bond at the junction between the blocks.

in the wet system. The center-of-mass motion is highly anisotropic, as expected.[2-5] Diffusion normal to the interface is opposed by the energetic barrier arising from the formation of additional A–B contacts when a block crosses the interface. Diffusion in the plane of the lamellae can occur without the net formation of A–B contacts and is therefore faster than motion normal to the interface.

Bond Autocorrelation Functions

The time autocorrelation functions of the bonds at the free ends and at the junction points have been calculated as

$$M(\tau) = \frac{1}{N_c t_{run}} \sum_{i=1}^{N_c} \sum_{t=1}^{t_{run}} \mathbf{m}(\tau+t)\cdot\mathbf{m}(t) \qquad (3)$$

where $\mathbf{m}(t)$ and $\mathbf{m}(\tau+t)$ are the bond vectors, of unit length, at time t and after time interval τ, respectively. The behavior of $M(\tau)$ is depicted in Figure 6. In both systems, $M(\tau)$ rapidly decays to zero when it is evaluated for the bonds at the free ends of the blocks. These bonds can easily sample all six directions that are available on the cubic lattice.

In contrast, $M(\tau)$ for the bonds at the junctions between the blocks rapidly decay only as far as $M(\tau) \sim 0.5$. Further decay takes place on a time scale much longer than the time of the simulation (at 6000 Monte Carlo time steps, $M(\tau)$ is 0.47 for the bonds at the junctions between the

blocks in the wet system). If the bond at the junction between the blocks were to randomize over the five positions that do not entail a complete reversal of the initial position, $M(\tau)$ would decay to 0.2. On the time scale of the simulation, not even this amount of disorder is produced in the bond at the junction between the two blocks. The strong tendency for orientation of the bond at the junction between the blocks in the simulations is consistent with recent results.[6,7,9]

Conclusions

The simulation of the dynamics of the lamellar phase of a diblock copolymer near the microphase separation transition shows that the components of the self-diffusion coefficient in the plane of the lamellae are an order of magnitude larger than the component normal to the plane. The bond autocorrelation functions decay rapidly to zero for the bonds at the free ends. In contrast, the autocorrelation function for the bond at the junction between the two blocks does not fall below 0.4–0.5 during the simulation, indicating a strong tendency for the retention of orientation near the interface.

Acknowledgment. This research was supported by National Science Foundation Grants DMR 89-15025 and DMR 90-14502 and by the NSF Center for the Molecular and Microstructure of Composites.

References and Notes

(1) Bates, F. S.; Fredrickson, G. H. *Annu. Rev. Phys. Chem.* **1990**, *41*, 525.
(2) Matsushita, Y.; Mori, K.; Saguchi, R.; Noda, I.; Nagasawa, T.; Chang, T.; Glinka, J.; Han, C. *Macromolecules* **1990**, *23*, 4387.
(3) Helfand, E. *Macromolecules* **1992**, *25*, 492.
(4) Dalvi, M. C.; Lodge, T. P. *Macromolecules* **1993**, *26*, 859.
(5) Mayes, A. M.; Johnson, R. D.; Russel, T. P.; Smith, S. D.; Satija, S. K.; Majkrzak, C. F. *Macromolecules* **1993**, *26*, 1047.
(6) Shull, K. R.; Kramer, E. J.; Bates, F. S.; Rosedale, J. H. *Macromolecules* **1991**, *24*, 1383.
(7) Barrat, J. L.; Fredrickson, G. H. *Macromolecules* **1991**, *24*, 6378.
(8) Fried, H.; Binder, K. *J. Chem. Phys.* **1991**, *94*, 8349.
(9) Balaji, R.; Wang, Y.; Foster, M. D.; Mattice, W. L. *Comput. Polym. Sci.* **1993**, *3*, 15.
(10) Wall, F. T.; Mandel, F. *J. Chem. Phys.* **1975**, *63*, 4592.
(11) Verdier, P. H.; Stockmayer, W. H. *J. Chem. Phys.* **1962**, *36*, 227.
(12) Metropolis, N.; Rosenbluth, A. N.; Rosenbluth, M. M.; Teller, A. H.; Teller, E. J. *J. Chem. Phys.* **1953**, *21*, 1087.